Comparison of different slug frequency calculation methods for the validation of two-phase flow simulations

S. Schmelter[1], S. Knotek[2], M. Olbrich[1,3], M. Bär[1]

[1]Physikalisch-Technische Bundesanstalt (PTB), Abbestr. 2-12, 10587 Berlin, Germany
[2]Czech Metrology Institute (CMI), Brno, Czech Republic
[3]Technische Universität Berlin, Berlin, Germany
E-mail (corresponding author): sonja.schmelter@ptb.de

Abstract

Slug flow is a common flow pattern, which is often accompanied by undesired effects, like pressure loss or vibrations, leading to large errors in multiphase flow metering. Because these undesired effects strongly correlate with the frequency of slug occurrence, this parameter is of special interest. In this paper, different slug frequency calculation methods are applied to data from multiphase flow simulations and corresponding high-speed video observations for six test cases within the plug / slug flow regime. Commonly used methods, like power spectral density (PSD) or calculating the mean slug frequency by applying a fixed threshold, are compared with new evaluation methods. Since every approach has its pros and cons, it is recommended to apply different methods to each data set. The deviations in the resulting slug frequencies indicate how much one can trust the results. If large variations are observed, one should apply an advanced technique for the calculation of the liquid level / hold-up, which takes aeration into account.

1. Introduction

The measurement of multiphase flows is of great importance in various applications in the nuclear, chemical, or oil and gas industries. Due to specific multiphase flow phenomena, such as different flow regimes, measuring multiphase flows is much more complex than single-phase flow metering. Numerical simulations of multiphase flows with different properties and different flow rates can help to quantify the influence of these flow conditions on the measurement process. The great advantage of computational fluid dynamics (CFD) is that it gives insight into areas that are hardly accessible by experiments. However, before CFD simulations can be used for predicting flows, they need to be validated.

The slug flow pattern is one of the most commonly observed two-phase flow patterns in industrial applications [1]. It is characterized by alternating blocks of aerated liquid (so-called slugs) and gas bubbles flowing above liquid films [2]. These liquid slugs can cause severe problems in industrial operations and lead to large uncertainties in multiphase flow metering [3]. Because these undesired effects strongly correlate with the frequency of slug occurrence [2], this parameter is of special interest.

In this paper, six different test cases within the plug and slug flow regime were simulated with the open-source software package OpenFOAM. The simulation results were validated by comparison with experimental data derived from high-speed video recordings of the flow from the side. The parameter of interest in these investigations was plug / slug frequency, which was determined by means of several calculation methods. The used approaches can be divided into two groups: methods based on thresholding and frequency analysis. In the literature, it is often not stated, which criteria a structure has to meet to be identified as a slug [4]. Furthermore, there are no uniform rules for the choice of appropriate thresholds in slug detection algorithms. Some authors propose fixed thresholds, see, e.g., [5], others applied variable ones, see, e.g., [6]. In this contribution, some commonly used methods for calculating the slug frequency from liquid level time series, like power spectral density (PSD) or calculating the mean slug frequency by applying a fixed threshold to the liquid hold-up, were compared with new evaluation methods proposed by the authors. Finally, guidance for choosing appropriate slug detection and slug frequency calculation methods is given.

2. Experimental and numerical set-up

This section introduces the test cases considered in this paper. Furthermore, the experimental and numerical set-up are described. For both, experimental data as well as simulation results, it is explained how liquid level time series are derived.

2.1 Experimental set-up

Experimental data of six different plug / slug flow test cases are analyzed to verify the results of the numerical simulations. The flow rates and observed flow patterns (differentiation between plug and slug flow is based on the flow pattern map by Mandhane et al. [7]) of these cases are given in Table 1. The fluid properties are summarized in Table 2.

Table 1: Flow rates and flow patterns of the different test cases.

Name of test case	Liquid flow rate in m³/h	Gas flow rate in m³/h	Flow pattern
TP 03 / 79	35	43	slug
TP 05 / 81	50	17	plug
TO 05 / 84	90	30	slug

Table 2: Properties of the different fluids.

Fluid property	Paraflex oil	Brine water	Nitrogen
Density in kg/m³	$8.16 \cdot 10^{2}$	$1.02 \cdot 10^{3}$	$1.08 \cdot 10^{1}$
Dynamic viscosity in Pa·s	$7.84 \cdot 10^{-3}$	$8.30 \cdot 10^{-4}$	$1.75 \cdot 10^{-5}$
Surface tension in N/m	$2.86 \cdot 10^{-2}$	$7.00 \cdot 10^{-2}$	-

The experiments were performed at TÜV SÜD National Engineering Laboratory (NEL) as part of the European research project “Multiphase flow reference metrology” [8]. The experimental set-up consisted of a straight horizontal pipe with inner diameter $D = 0.097\ \mathrm{m}$ and a length of approximately $10\ \mathrm{m}$, followed by a transparent Perspex viewing section with a length of $0.5\ \mathrm{m}$, where the flow pattern was recorded from the side by a high-speed video camera. For further details, the reader is referred to [9].

2.2 Numerical set-up

For a better assessment of the development of plug / slug flow, a longer pipe ($L = 20\ \mathrm{m} \approx 206D$) than in the experiment is considered in the numerical simulations, see Figure 1.

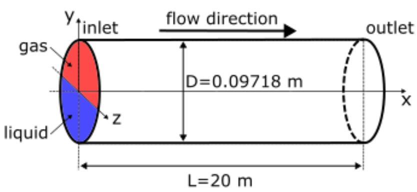

Figure 1: Illustration of the geometry, initial and boundary conditions used in the numerical simulations.

The multiphase flow simulations were performed using the software package OpenFOAM-5.x. From this package, the two-phase solver *interFoam* was chosen, which is based on the volume of fluids (VOF) method [10]. Turbulence was modeled by means of Reynolds-averaging the Navier-Stokes equations and applying the shear stress transport (SST) model [11]. For the numerical simulations, a hexahedral mesh consisting of approximately 3.5 million cells was designed for one half of the geometry with a symmetry plane in the *y*-axis, see Figure 1. This mesh proofed to be a good compromise between time expenses and accuracy, see [9,12] for further details. The inlet cross section was bisected horizontally as shown in Figure 1. Through the upper part, the gas enters the pipe, whereas the liquid enters the pipe through the lower part. For both parts, an inflow boundary condition was used prescribing the corresponding velocities of the phases in flow direction. Since these simplified boundary conditions cause less irregular dynamics than present in reality, random perturbations of the secondary components of the velocity vectors at the inlet as proposed in [9] are used. At the outlet, a constant pressure boundary condition was applied. The walls of the pipe were treated as hydraulically smooth with no-slip boundary conditions for both phases. The contact angle was set to 72°. For the time discretization, the implicit Euler scheme was used. The time step size was adjusted automatically by limiting the Courant number to 0.5. Further details on the numerical schemes can be found in [9].

2.3 Extraction of liquid level time series

For the validation of the simulation results with experimental data, liquid level time series are considered. According to Andritsos and Hanratty [13], the liquid level is defined as the vertical position of the gas-liquid interface relative to the inner diameter in the vertical centerline of the pipe cross section.

For the experimental data, the liquid level time series are extracted from high-speed video observations, which represent a two-dimensional projection of the three-dimensional flow from the side. To extract the liquid level time series from the video, an image processing routine is used [14]. Since the flow is observed through a relatively thick transparent pipe wall, the liquid level observed from outside is distorted compared to the real liquid level. Hence, a correction based on Snell-Descartes law and trigonometry is applied, see [15] for details. Note that, in the videos, only 94 % of the pipe are visible due to the construction of the Perspex viewing section. The lowest and highest 3 % of the pipe cannot be seen because of tie bars that were needed for the installation. Nevertheless, the liquid level time series extracted from these observations represent the dynamics of the gas-liquid interface and reveal the temporal characteristics of the flow structures. Hence, they can be used for the calculation of slug frequency.

From the simulation results, the liquid level time series at a fixed downstream position *x* and time *t* are approximated as follows:

$$h_L(x,t) \approx h_L^{\text{sim}}(x,t) = \frac{1}{D}\int_{-D/2}^{D/2} \alpha(t,x,y,z=0)dy,$$

where α denotes the liquid volume fraction.

3. Slug frequency calculation methods

Slug frequency is defined as the number of slugs that passes a specific point along the pipeline over a certain period of time [16]. For the detection of slugs from the liquid level time series, different methods can be used. They can be divided into two groups: one approach is based on defining thresholds for slug detection, the other one uses frequency analysis.

3.1 Methods based on thresholding

According to the definition of a slug as a block of (aerated) liquid passing through the pipe, see Figure 2 (left), the detection of slugs is often based on thresholding. Whenever the liquid level raises above a certain threshold value, a slug is counted. This procedure is illustrated in Figure 2 (right).

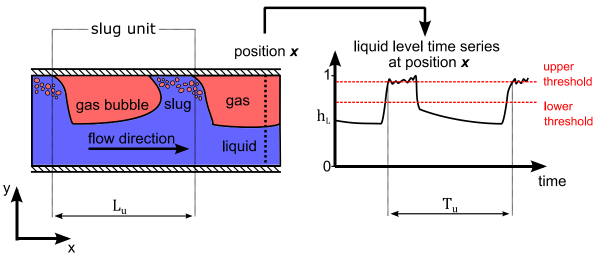

Figure 2: Illustration of a slug unit (left) and corresponding liquid level time series, as well as chosen thresholds for slug detection (right).

In theory, this upper threshold should be close to one. In practice, however, slugs are often distorted and aerated (so that the interface between liquid and gas is less distinct), which means that the choice of an appropriate threshold value can become difficult. In this contribution, we used a threshold of 0.9. Furthermore, we investigated the influence of increasing and decreasing the threshold to 0.95 and 0.85, respectively. Additionally, a lower threshold was introduced, which avoids the double-counting of slugs due to small fluctuations in the liquid level. Here, the mean liquid level was used as lower threshold. Hence, a slug is only counted if the liquid level raises above the upper threshold after having been below the lower threshold before. A detailed study on the sensitivity of slug frequency on the choice of both, upper and lower, thresholds can be found in [4].

After having determined all the slugs in the considered time interval, the mean slug frequency can be defined as follows:

$$\overline{f_s} = \frac{\text{number of slugs}}{\text{length of time interval}}.$$

Furthermore, the slug unit time T_u, i.e., the time difference between two consecutive slugs, see Figure 2 (right), can be considered. Figure 3 shows a histogram (blue bars) for the probability density estimate of T_u for TP 03 at position $x = 200D$. Please note that the width of the distribution describes how regularly slugs occur.

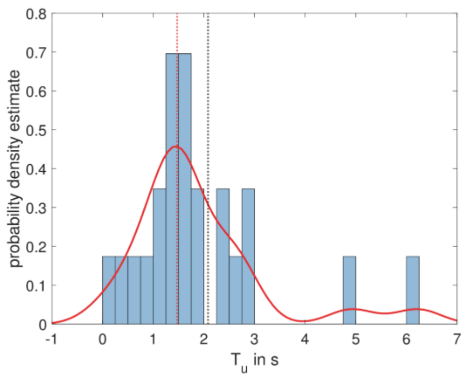

Figure 3: Histogram and kernel fit of the probability density estimate of $\boldsymbol{T_u}$ for TP 03 at $x = 200D$.

Furthermore, a kernel fit was applied (solid red line). The mode of the corresponding distribution (dotted red line) represents the most probable time difference between two consecutive slugs. For comparison, the inverse of the mean slug frequency is also plotted in this graph (dotted black line). Compared to the mode of the distribution, this value is much higher because it also takes the seldomly occurring large time differences (of approximately five and six seconds) into account. Figure 4 shows the histogram (blue bars) as well as the fitted kernel distribution (solid red line) of the probability estimate for T_u^{-1}.

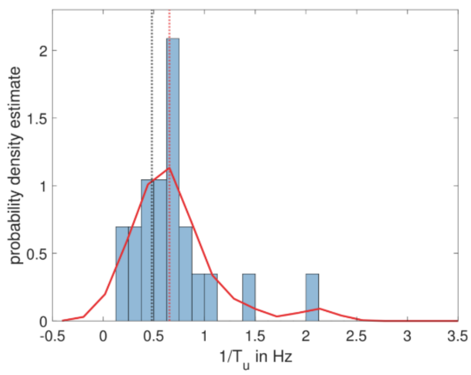

Figure 4: Histogram and kernel fit of the probability density estimate of $\boldsymbol{T_u^{-1}}$ for TP 03 at $x = 200D$.

The mode of the distribution, which can be interpreted as the most probable frequency of consecutive slugs, is plotted as a dotted red line.

Again, the mean slug frequency is shown for comparison (dotted black line).

By means of the modes of the distributions of T_u and T_u^{-1}, *peak slug frequency* $\hat{f}_s$ and *inverse peak slug frequency* $\check{f}_s$ are defined as follows:

$$\hat{f}_s = \frac{1}{\arg\max p(T_u)}, \qquad \check{f}_s = \arg\max q(T_u^{-1}),$$

where $p(\cdot)$ and $q(\cdot)$ denote the fitted kernel distribution functions of the probability density estimates for T_u and T_u^{-1}, respectively.

3.1 Methods based on frequency analysis

Another commonly used method to estimate the frequency of slug occurrence is the calculation of the PSD of the liquid holdup or liquid level time series, see, e.g., [5,6,17]. This approach has the advantage that it is easy to apply and that no thresholds need to be chosen. On the other hand, the most dominant frequencies determined by a PSD are not necessarily the frequencies of the slugs, but only reflect the dynamics of the interface between the different phases [9,12]. For the investigations in this paper, not only PSD but also Welch's power spectral density estimate (calculated with the function *pwelch* in Matlab) was applied. The latter one uses additional smoothing, making it more robust than a pure Fourier transform. The parameters for *pwelch* were chosen as in [9].

4. Results and discussion

In this section, the two newly introduced parameters, peak slug frequency and inverse peak slug frequency, are presented for all six considered test cases. Furthermore, the results derived with these slug frequency calculation methods are compared with classical approaches, namely PSD, *pwelch*, and mean slug frequency, as well as with a slug frequency that has been derived by visually counting the slugs in the videos. This value can serve as a reference although it has the disadvantage that it is prone to subjective judgement.

Figures 5 and 6 show the peak slug frequencies at different downstream positions $90D \le x \le 200D$ derived from the CFD simulations for the oil-gas and water-gas test cases, respectively. The corresponding experimental data derived from the video observations at position $x \approx 103D$ are plotted for comparison. For the oil-gas test cases, good agreement between simulation results and experimental data can be observed. For the water-gas test cases, on the other hand, the peak slug frequencies observed in the experiments at position $x \approx 103D$ do not fit very well to the simulated peak slug frequencies at this position, but much better to the peak slug frequencies observed further downstream in the pipe at $x = 140D$ or $x = 160D$.

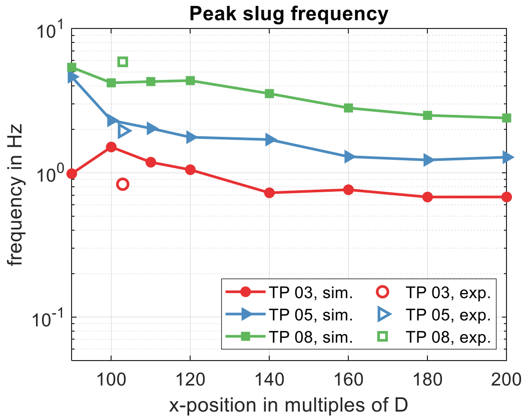

Figure 5: Peak slug frequency $\hat{f}_s$ at different downstream positions $90D \le x \le 200D$ for oil-gas test points.

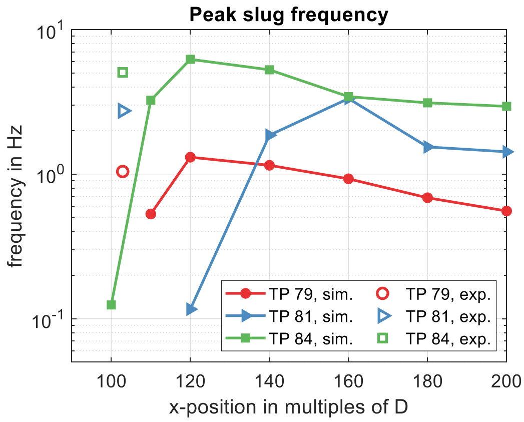

Figure 6: Peak slug frequency $\hat{f}_s$ at different downstream positions $90D \le x \le 200D$ for water-gas test points.

Please note that missing positions in the simulation results in Figure 6 indicate that no slugs have been observed at these positions (i.e., for $x \le 100D$ for TP 79, $x \le 110D$ for TP 81, and $x \le 90D$ for TP 84). Altogether, it can be concluded that, for the water-gas test cases, the formation of slugs in the numerical simulations takes much longer than in the corresponding experiment. One approach to overcome this problem is to use a higher value for the perturbation parameter in the numerical simulations, see [9].

Figures 7 and 8 show the inverse peak slug frequencies for oil-gas and water-gas test points, respectively. Similar observations can be made as for the peak slug frequencies: For the oil-gas test cases, the agreement between simulation results and experimental data is quite good, whereas, for the water-gas test cases, the simulation results need to be evaluated at positions further downstream than the corresponding experimental data. Again, these deviations can be explained by the simplified boundary conditions used in the numerical model. As discussed in [9], these boundary conditions introduce less turbulence into the system than present in reality.

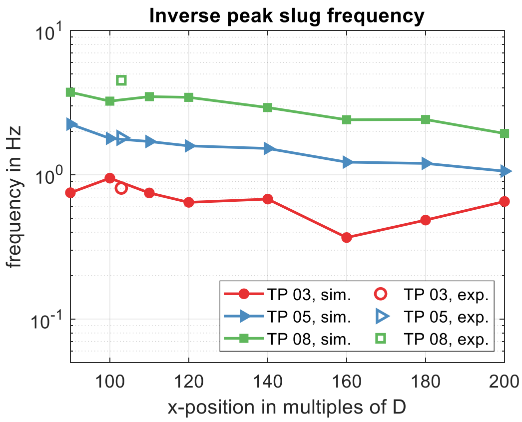

Figure 7: Inverse peak slug frequency $\check{f}_s$ at different downstream positions $90D \leq x \leq 200D$ for oil-gas test points.

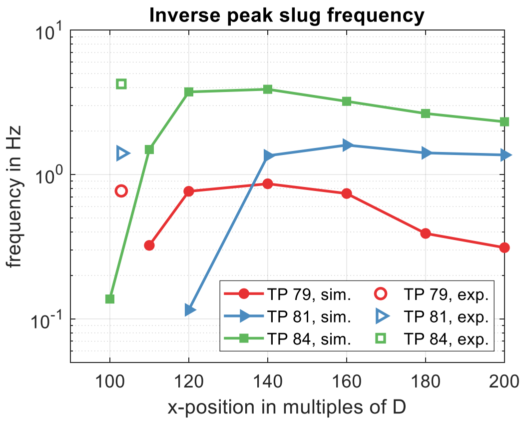

Figure 8: Inverse peak slug frequency $\check{f}_s$ at different downstream positions $90D \leq x \leq 200D$ for water-gas test points.

Figure 9 shows a comparison of the different slug frequency calculation methods for all test points. To get a flow pattern that is as much developed as possible, the simulation results were evaluated at $x = 200D$ for this comparison. Note that the corresponding experimental data were nevertheless obtained at $x \approx 103D$. For the methods that are based on thresholds for slug detection, also the sensitivity of this parameter has been investigated. The range of frequencies observed for thresholds varied between 0.85, 0.9, and 0.95 is indicated by error bars in the figure.

For some test cases (e.g., the simulated cases TP 05, TP 81, and TP 84), hardly any difference in the resulting slug frequencies can be observed for the different approaches. These cases also show hardly any sensitivity with respect to the chosen threshold for slug detection. In contrast, there are some other cases (e.g., the simulated cases TP 79 or TP 08), which are very sensitive to the choice of the threshold. There are several reasons for this sensitivity. One reason is that, due to aeration in the liquid phase, slugs are not detected because the threshold is chosen too small. This problem can be avoided by lowering the threshold for slug detection according to the ratio of gas present in the slugs. Alternatively, a different method for the extraction of the liquid level time series can be used, which takes aeration into account, see [4] for details. Another reason is that, due to small fluctuations in the liquid level, one slug structure is counted several times. To avoid this, a second (lower) threshold was introduced in Section 3.1. For cases with a relatively high (mean) liquid level, however, this problem can still occur. An approach to overcome this problem is to ignore slug unit times that are below a certain threshold. In [18], a procedure for the automatic detection of these time

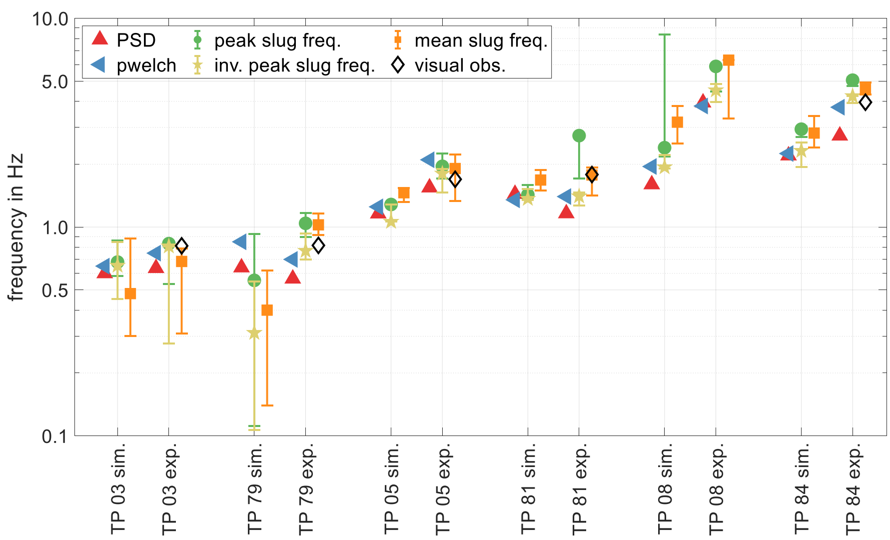

Figure 9: Comparison of different slug frequency calculation methods: PSD, *pwelch*, peak slug frequency, inverse peak slug frequency, mean slug frequency, and slug frequency determined by visual observation. The error bars indicate the range of frequencies observed if the threshold for slug detection is varied between 0.85, 0.9, and 0.95.

scales is presented.

A comparison between simulation results and experimental data shows quite good agreement for most of the test cases. Only for TP 79 and TP 08, where the simulation results are very sensitive to the applied slug frequency calculation method, the frequencies calculated from the CFD results are significantly smaller than the ones derived from the experimental data. Hence, it seems to be a good strategy to apply different slug calculation methods (and also different thresholds) in order to assess the variation of the results. In case of strongly varying slug frequencies, it is recommended to use some advanced techniques for the extraction of the liquid level time series as well as for slug detection as discussed above.

5. Conclusion

In this paper, different slug frequency calculation methods have been applied to data from multiphase flow simulations on one hand and from experimental video observations on the other hand. The overall agreement between simulation results and experimental data was quite good. Nevertheless, for some cases, where the calculated slug frequencies were highly sensitive to the chosen method and threshold, deviations could be observed. For these cases, it is recommended to use advanced techniques for slug detection, which are able to take aeration into account.

Acknowledgement

This work was supported through the Joint Research Project "Multiphase flow reference metrology". This project has received funding from the EMPIR programme co-financed by the Participating States and from the European Union's Horizon 2020 research and innovation programme.

References

[1] Pineda-Pérez H, Kim T, Pereya E, Ratkovich R, "CFD modeling of air and highly viscous liquid two-phase slug flow in horizontal pipes", *Chem. Eng. Res. Des.,* **136**, 638–653, 2018.

[2] Al-Safran E M, "Investigation and prediction of slug frequency in gas/liquid horizontal pipe flow", *J. Pet. Sci. Eng.,* **69**, 143–155, 2009.

[3] Olbrich M, Bär M, Oberleithner K, Schmelter S, "Statistical characterization of horizontal slug flow using snapshot proper orthogonal decomposition", *Int. J. Multiph. Flow*, **134**, 103453, 2021.

[4] Webner F, Polansky J, Knotek S, Schmelter S, "Sensitivity analysis of threshold parameters in slug detection algorithms" [manuscript submitted for publication], 2022.

[5] Hernandez-Perez V, Abdulkadir M, Azzopardi B J, "Slugging frequency correlation for inclined gas-liquid flow", *Int. J. Chem. Mol. Eng.*, **4**, 10–17, 2010.

[6] Zhao Y, Yeung H, Lao L, "Slug frequency in high viscosity liquid and gas flow in horizontal pipes", in *16th Int. Conference on Multiphase Production Technology* (OnePetro), 2013.

[7] Mandhane J, Gregory G, Aziz K, "A flow pattern map for gas-liquid flow in horizontal pipes", *Int. J. Multiph. Flow*, **1**, 537–553, 1974.

[8] EURAMET, EMPIR project "Multiphase flow reference metrology", https://www.euramet.org/research-innovation/search-research-projects/details/project/multiphase-flow-reference-metrology/

[9] Schmelter S, Knotek S, Olbrich M, Fiebach A, Bär M, "On the influence of inlet perturbations on slug dynamics in horizontal multiphase flow – a computational study", *Metrologia*, **58**, 014003, 2021.

[10] Hirt C W, Nichols B D, "Volume of fluid /VOF/ method for the dynamics of free boundaries", *J. Comput. Phys.*, **39**, 201–225, 1981.

[11] Menter F R, "Two-equation eddy-viscosity turbulence models for engineering applications", *AIAA J.*, **32**, 1598–1605, 1993.

[12] Knotek S, Schmelter S, Olbrich M, "Assessment of different parameters used in mesh independence studies in two-phase slug flow simulations", *Measurement: Sensors*, **18**, 100317, 2021.

[13] Andritsos N, Hanratty T J, "Influence of interfacial waves in stratified gas-liquid flows", *AIChE J.*, **33**, 444–454, 1987.

[14] Olbrich M, Schmeyer E, Riazy L, Oberleithner K, Bär M, Schmelter S, "Valdation of simulations in multiphase flow metrology by comparison with experimental video observations", *J. Phys. Conf. Ser.*, **1065**, 092015, 2018.

[15] Schmelter S, Olbrich M, Schmeyer E, Bär M, "Validation of multiphase flow simulations by comparison with experimental video observations", in *North Sea Flow Measurement Workshop*, 2018.

[16] Al-Safran E M, "Investigation and prediction of slug frequency in gas/liquid horizontal pipe flow", *J. Pet. Sci. Eng.*, **69**, 143–155, 2009.

[17] Heywood N, Richardson J F, "Slug flow of air-water mixtures in a horizontal pipe: Determination of liquid holdup by γ-ray absorption", *Chem. Eng. Sci.*, **34**, 17–30, 1979.

[18] Soto-Cortes G, Pereyra E, Sarica C, Torres C, Soedarmo A, "Signal processing for slug flow analysis via a voltage or instantaneous liquid holdup time-series", *Flow Meas. Instrum.*, **79**, 101968, 2021.